

Electronic Supplementary Information

Novel Multielement Nanocomposite with Ultrahigh Rate Capacity and Durable Performance for Sodium-Ion Battery Anode

Xiaochuan Ren,^{‡^{a,b}} Yuanxin Zhao,^{‡^a} Qingwei Li,^c Feng Cheng,^b Wen Wen,^a Lili Zhang,^a Yaobo Huang,^a Xinhui Xia,^d Xiaolong Li,^a Daming Zhu,^{*a} Kaifu Huo,^{*b} and Renzhong Tai^a

^a Shanghai Synchrotron Radiation Facility, Shanghai Advanced Research Institute, Chinese Academy of Sciences, Shanghai 201204, China

^b Wuhan National Laboratory for Optoelectronics (WNLO), Huazhong University of Science and Technology, Luoyu Road 1037, Wuhan 430074, China

^c Advanced Research Institute for Multidisciplinary Science, Qilu University of Technology (Shandong Academy of Sciences), Jinan 250353, China

^d State Key Laboratory of Silicon Materials, Key Laboratory of Advanced Materials and Applications for Batteries of Zhejiang Province, Zhejiang University, Hangzhou, 310027, China

* Corresponding author: zhudaming@zjlab.org.cn; kfhuo@hust.edu.cn

[#] These authors contributed equally to this work.

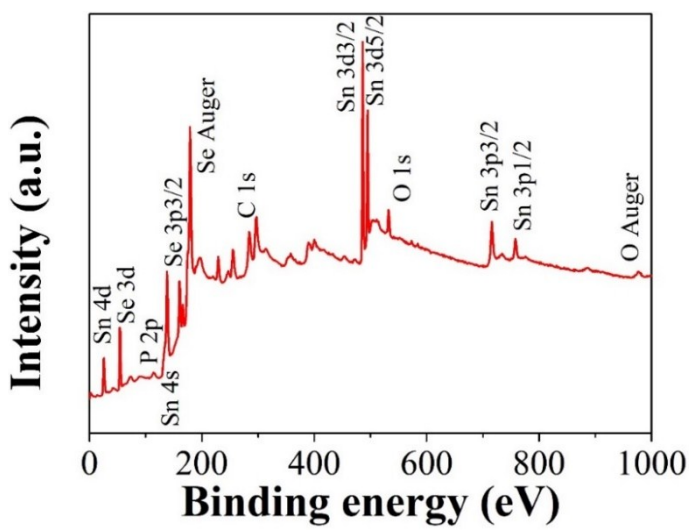


Fig. S1. The survey XPS spectrum of $\text{SnPSe}_3@\text{G}$.

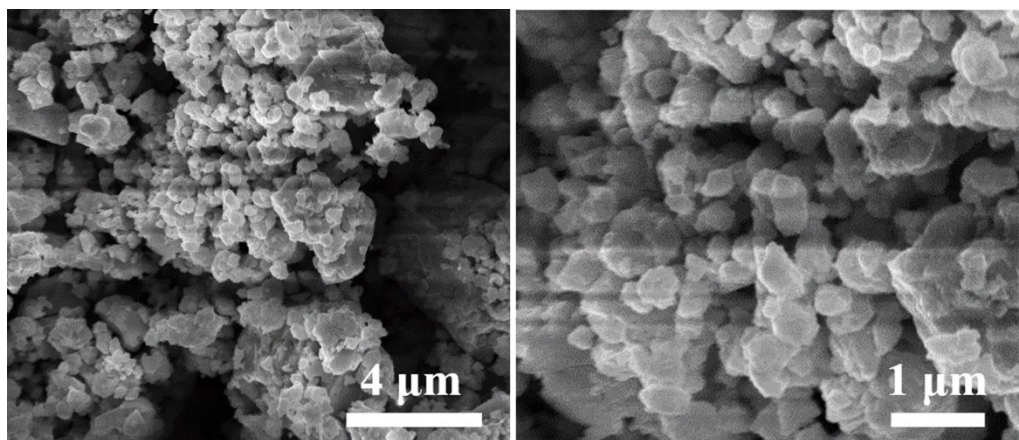


Fig. S2. SEM image of SnPSe₃.

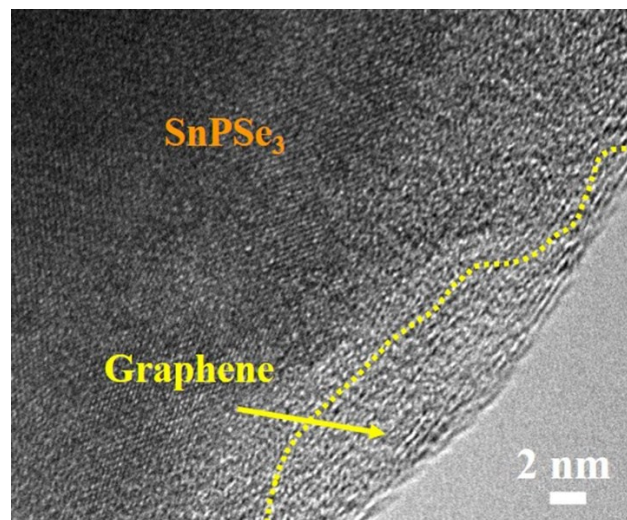


Fig. S3. (a) High-magnification TEM image of SnPSe₃@G composite.

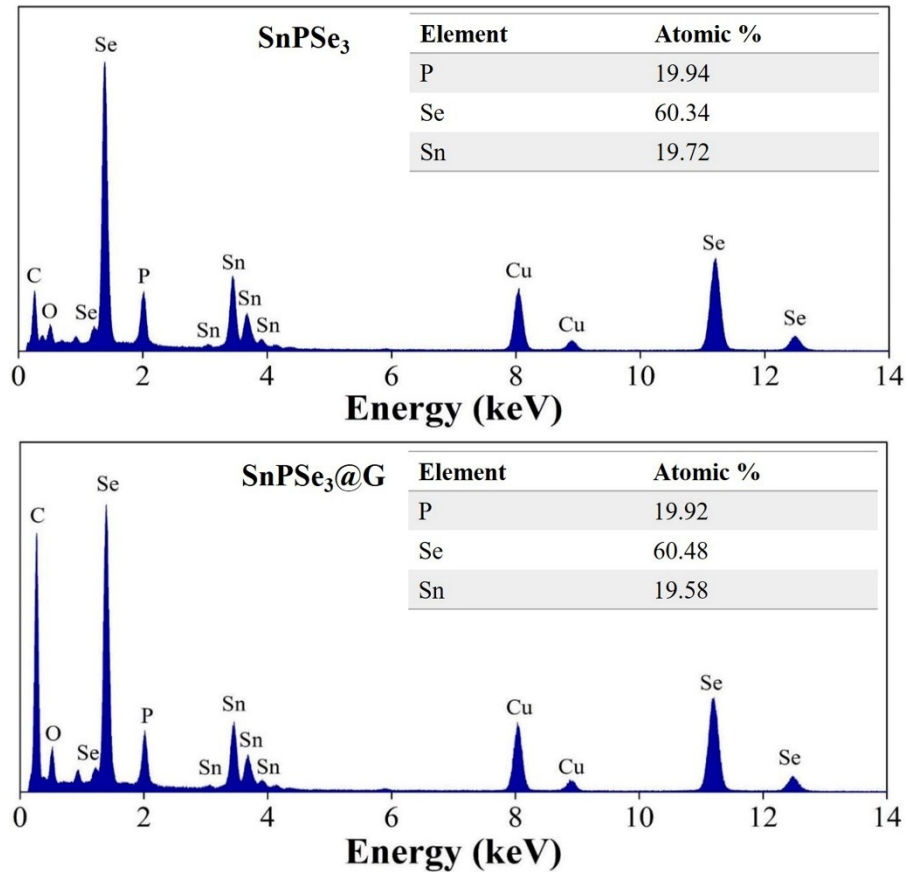


Fig. S4. EDX spectra of SnPSe_3 and $\text{SnPSe}_3@\text{G}$.

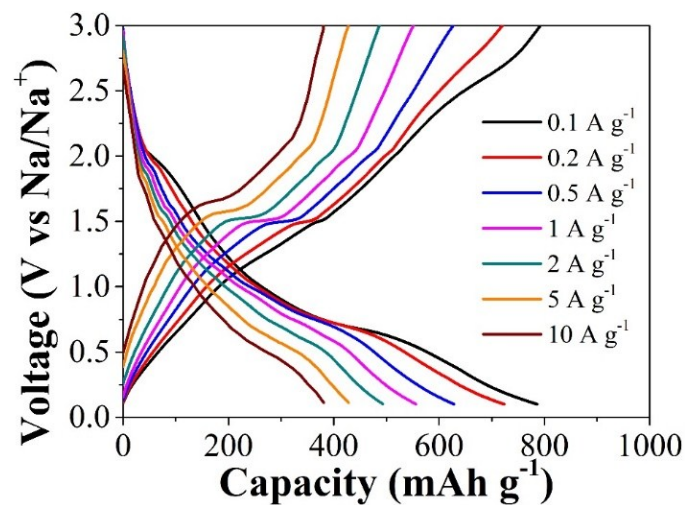


Fig. S5. Corresponding charge-discharge curves of SnPSe₃@G in NSF-M electrolyte at various current densities.

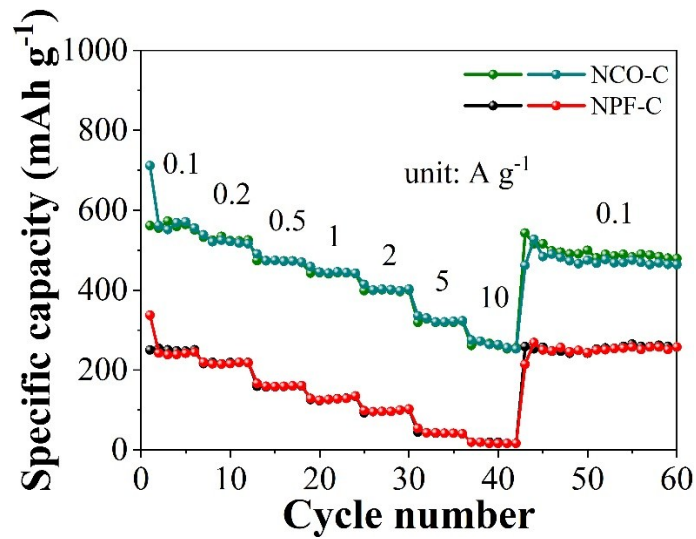


Fig. S6. Rate performance of $\text{SnPSe}_3@\text{G}$ in different electrolytes at a voltage window between 0.1-3.0 V.

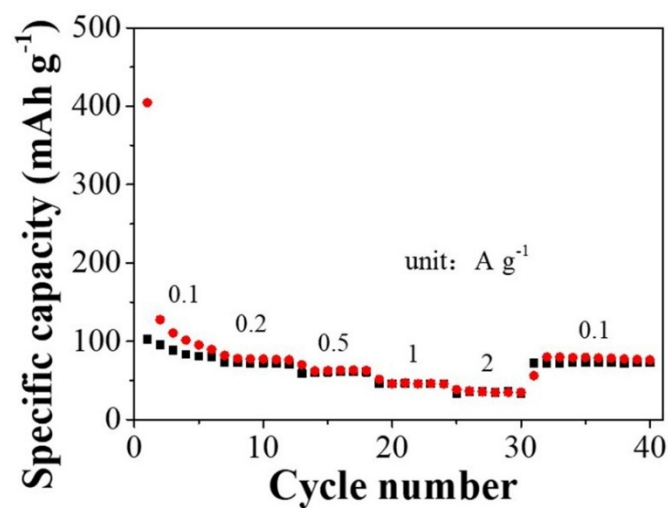


Fig. S7. Rate capability of the graphene electrode.

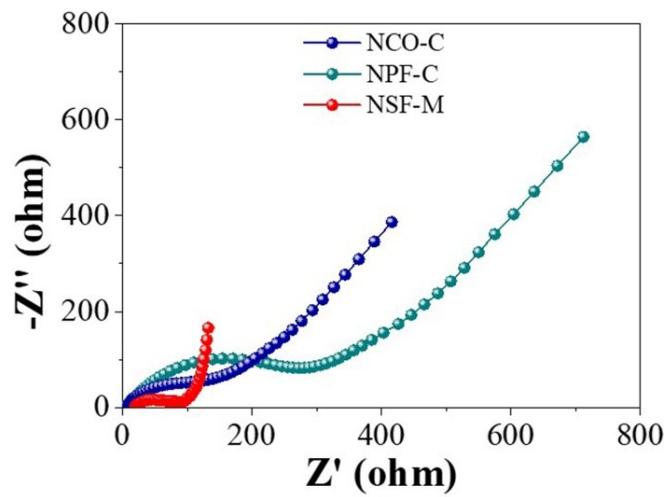


Fig. S8. Nyquist plots of $\text{SnPSe}_3@\text{G}$ in different electrolytes at the voltage window between 0.1-3.0 V

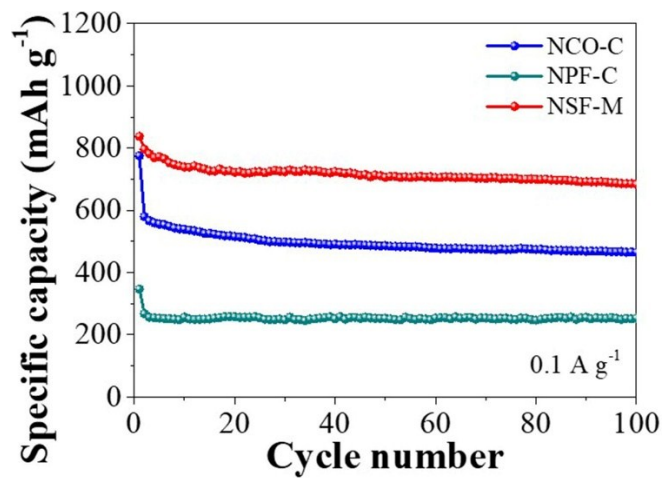


Fig. S9. Cycling stabilities of SnPSe₃@G in different electrolytes at 0.1 A g⁻¹.

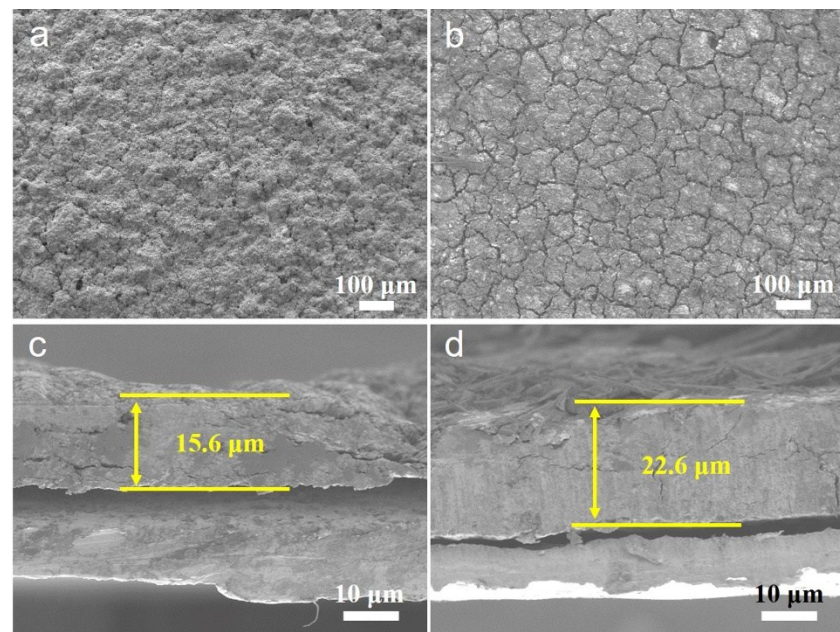


Fig. S10. The SEM images of the surface and cross-section morphology of SnPSe₃@G electrode before (a, c) and after (b, d) 100 cycles at 0.1-3 V.

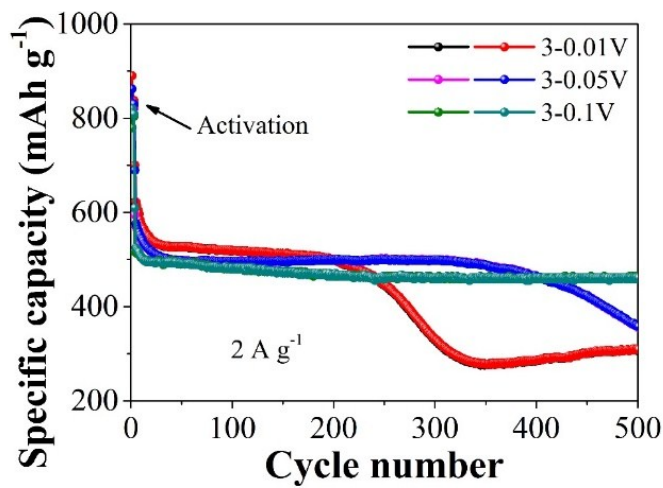


Fig. S11. The cycling performance of the $\text{SnPSe}_3@\text{G}$ electrode at 2 A g^{-1} with the different cut-off voltages in NSF-M electrolyte.

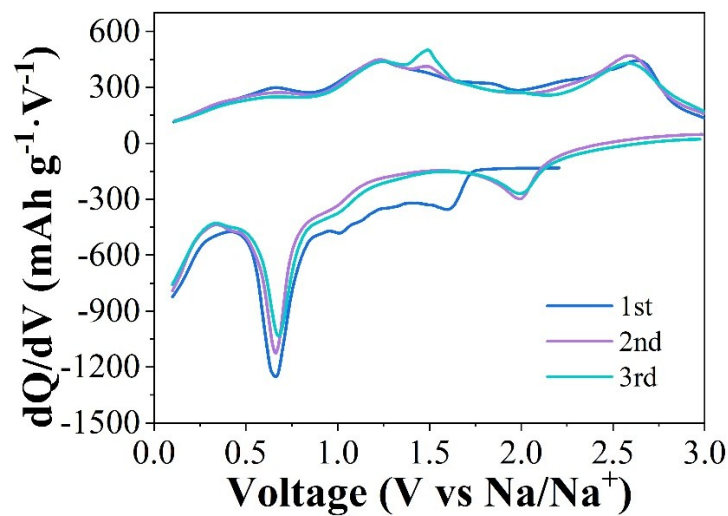


Fig. S12. Differential capacity (dQ/dV) vs. voltage plots of $\text{SnPSe}_3@\text{G}$ electrode for the initial three cycles in NSF-M electrolyte.

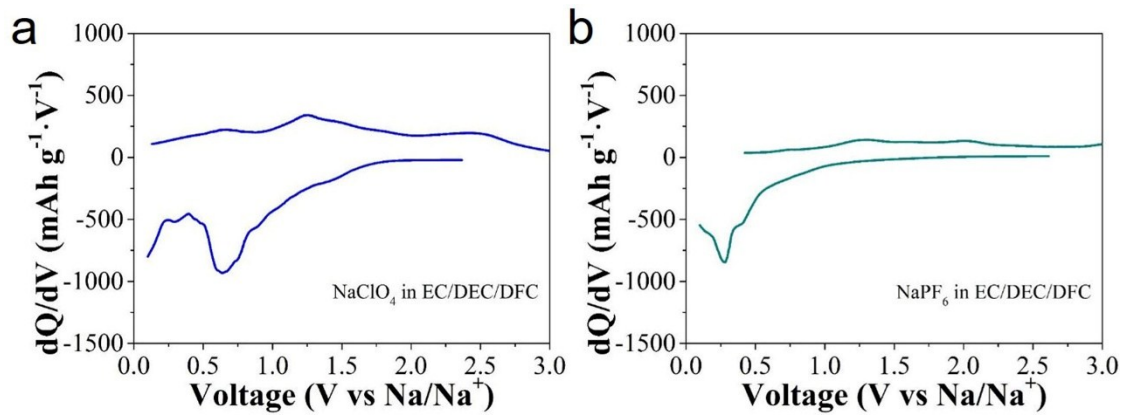


Fig. S13. Differential capacity (dQ/dV) vs. voltage plots in NCO-C (a) and NPF-C (b) electrolytes.

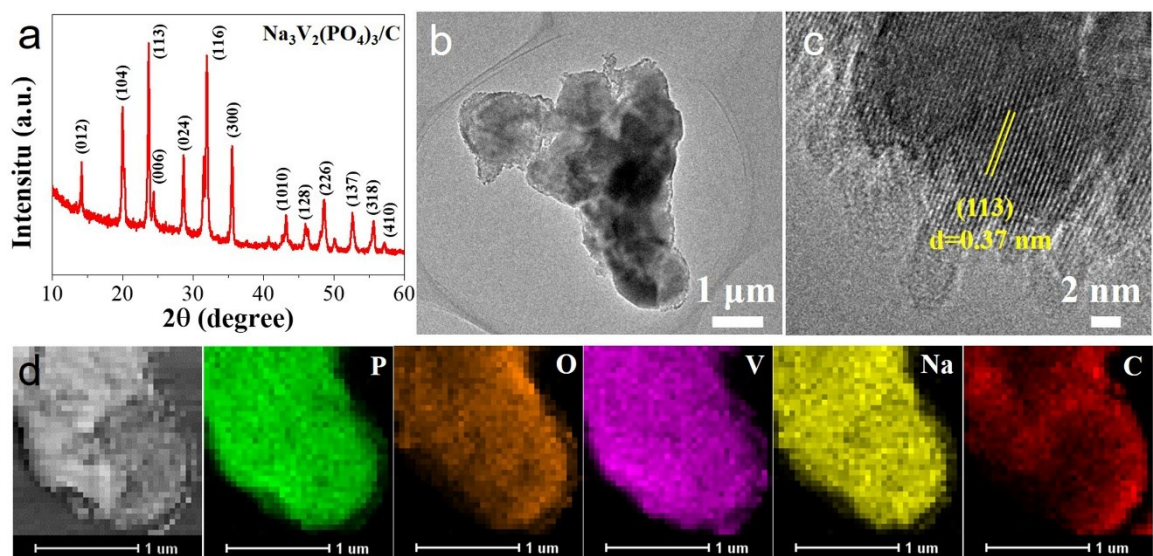


Fig. S14. (a) XRD, (b) TEM, (c) HRTEM and (d) EDX mapping of $\text{Na}_3\text{V}_2(\text{PO}_4)_3/\text{C}$ used as the cathode for sodium full-cell.

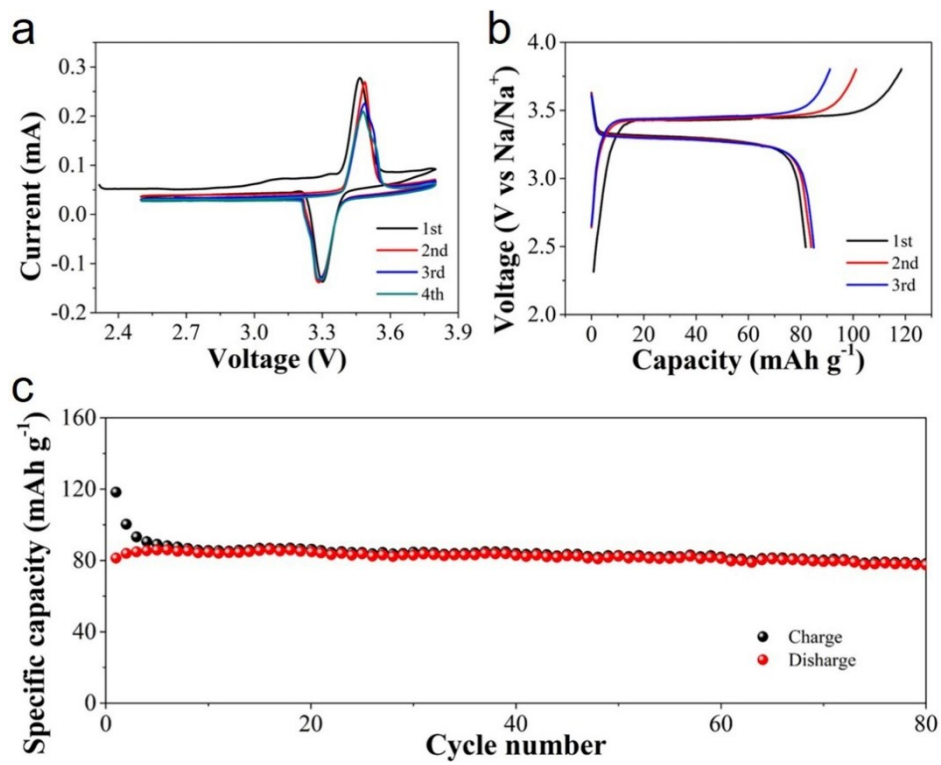


Fig. S15. Electrochemical performance of $\text{Na}_3\text{V}_2(\text{PO}_4)_3/\text{C}$ (NVP/C) as a cathode for sodium full-cell. (a) CV curves of the first four cycles at 0.2 mV s^{-1} in 2.5-3.8 V. (b) charge/discharge profiles and (c) cycling performance at 0.2 A g^{-1} between 2.5-3.8 V.

Table S1. The initial coulombic efficiency (ICE) comparisons of SnPSe₃@G electrode with the reported Sn-, Se- or P-based anodes for SIBs.^a

Electrode	Electrolyte	Initial coulombic efficiency	Ref.
Sn ₄ P ₃ @C	1 M NaPF ₆ in DME	90.7%	1
FeP/C	1 M NaPF ₆ in EC/DEC with 2% FEC	68.4%	2
Sandwich-like Ni ₂ P	1 M NaCF ₃ SO ₃ in TGM	69%	3
SnS ₂ @CNTs	1 M NaClO ₄ in EC/DEC with 5% FEC.	74.3%	4
FeSe ₂ @N-doped Carbon	NaCF ₃ SO ₃ in diglyme	97%	5
MoSe ₂ @C	1 M NaClO ₄ in PC with 5% FEC	75.7%	6
Sn ₄ P ₃ @porous carbon	1 M NaPF ₆ in EC/DMC with 10% FEC	72.5%	7
CoSe ₂ @B and N co-doped graphene	1 M NaCF ₃ SO ₃ in DEG/DME	68.5%	8
SnS ₂ /CNT	1 M NaPF ₆ in PC with 2% FEC	54%	9
SnPSe₃@G	1 M NaCF₃SO₃ in diglyme	95%	This work

^a DME: 1,2-Dimethoxyethane. EC: ethylene carbonate. DEC: diethylene carbonate. FEC: fluoroethylene carbonate. TGM: tetraethylene glycol dimethyl ether. PC: propylene carbonate. DMC: dimethyl carbonate. DEG: diethylene glycol.

References

1. X. Fan, T. Gao, C. Luo, F. Wang, J. Hu and C. Wang, *Nano Energy*, 2017, **38**, 350-357.
2. Y. Von Lim, S. Huang, Y. Zhang, D. Kong, Y. Wang, L. Guo, J. Zhang, Y. Shi, T. P. Chen, L. K. Ang and H. Y. Yang, *Energy Storage Mater.*, 2018, **15**, 98-107.
3. C. Dong, L. Guo, Y. He, C. Chen, Y. Qian, Y. Chen and L. Xu, *Energy Storage Mater.*, 2018, **15**, 234-241.
4. Y. Liu, X.-Y. Yu, Y. Fang, X. Zhu, J. Bao, X. Zhou and X. W. Lou, *Joule*, 2018, **2**, 725-735.
5. P. Ge, H. Hou, S. Li, L. Yang and X. Ji, *Adv. Funct. Mater.*, 2018, **28**, 1801765.
6. P. Ge, H. Hou, C. E. Banks, C. W. Foster, S. Li, Y. Zhang, J. He, C. Zhang and X. Ji, *Energy Storage Mater.*, 2018, **12**, 310-323.
7. L. Ran, I. Gentle, T. Lin, B. Luo, N. Mo, M. Rana, M. Li, L. Wang and R. Knibbe, *J. Power Sources*, 2020, **461**, 228116.
8. H. Tabassum, C. Zhi, T. Hussain, T. Qiu, W. Aftab and R. Zou, *Adv. Energy Mater.*, 2019, **9**, 1901778.
9. Z. Liu, A. Daali, G. L. Xu, M. Zhuang, X. Zuo, C. J. Sun, Y. Liu, Y. Cai, M. D. Hossain, H. Liu, K. Amine and Z. Luo, *Nano Lett.*, 2020, DOI: 10.1021/acs.nanolett.0c00964.